Latin American Journal of Solids and Structures
www.lajss.org

An Empirical Study on Ballistic Resistance of Sandwich Targets with Aluminum Facesheets and Composite Core

Abstract

This study attempted to examine the ballistic resistance of sandwich structures with aluminum facesheets, polyurethane core and polyurethane foam reinforced with aluminum pins. The main focus was on the effect of variations in density of core foam and the effect of adding different percentages of aluminum pins on energy absorption and ballistic resistance of sandwich structures under the impact of blunt and conical nose projectiles at high velocities (170 to 260 m/s). The results firstly demonstrated that any increase in the density of foam led to greater energy absorption. Secondly, the ballistic limit of sandwich structures with composite core was more than the foam core by 18 percent. Thirdly, the use of aluminum pins not only enhanced core resistance, but also altered the shape of damage and energy absorption in the rear facesheet. Finally, the ballistic limit of blunt projectile was greater than that of conical nose projectile.

Keywords

ballistic resistance, foam, sandwich structures, composite core

A. Alavi Nia [a]
H. Ranjbarzadeh [b]
M. Kazemi [c,*]

[a]Department of Mechanical Engineering, Bu-Ali Sina University, Hamedan, Iran.
[b]Master of Science, Mechanical Engineering.
[c]PhD Student, Mechanical Engineering, Bu-Ali Sina University, Hamedan, Iran.

* Corresponding author:
kazemii.m@gmail.com

http://dx.doi.org/10.1590/1679-78253390

Received 21.09.2016
In revised form 21.04.2017
Accepted 23.04.2017
Available online 25.04.2017

1 INTRODUCTION

Polymer-textured composite sheets and sandwich structures are largely used in thec transportation, marine, military and aerospace industries due to their low weight, corrosion resistance and high strength against impact loading. Moreover, they entail several applications in aircrafts, ships, vehicles, wind power systems and bridges.

Higher energy absorption under impact loading can deform the material in sandwich structures, particularly when the core comprises lightweight cellular material. Cellular structures are capable of withstanding large plastic deformation under a constant stress known as plateau stress. Hence, they can absorb great amounts of kinetic energy before collapsing (Dean, S-Fallah et al. 2011). These materials are most ideal and functional when exposed to stresses approximate to their plateau stress level. Compressive stress-strain curves of these materials can be divided into three regimes: linear-

elastic, yield plateau with approximately zero slope (plateau stress), and a final portion of steeply rising stress. The strain corresponding to the onset of the rapidly rising portion of the stress-strain curve is labeled as the densification strain.

In recent years, many empirical studies have been conducted on the effects of impact on a sandwich structure. A few of such studies explored the behavior of structures against high velocity impact (Nasirzadeh and Sabet 2014). The majority of studies focused on sandwich structures with honeycomb or PVC core in order to identify failure load, ballistic limit velocity, penetration energy and the extent of damage zone caused by collision with a projectile (Belingardi, Cavatorta et al. 2003). Goldsmith and Sackman (1992) conducted experimental studies on sandwich structures with honeycomb core and composite facesheets under static and dynamic loadings. Reyes et al. (2003) examined the use of sandwich structures in the industry. According to the results of tests, they suggested three failure modes for the structure in quasi-static compression, covering a local indentation inside the impact zone, shear deformation of the core and compressive facesheet deformation. Mines et al. (1998) studied and tested sandwich structures with composite facesheet and honeycomb core under low-velocity impact. They observed that energy absorption was enhanced by increasing the incident velocity of the projectile. This result was referred to an increase in core bearing stress, cracks and failures in the core and facesheet at high strain rates. Roach et al. (1998) investigated the penetration energy under static and dynamic modes in sandwich structures with PVC closed cell foam core and also studied the relationship between the amount of absorbed energy and the extent of delamination in sandwich structures. Alavi Nia and Kazemi (2015) analyzed high velocity impact on sandwich panels with metal facesheets and foam core in normal impact with a cylindrical projectile. In order to evaluate the accuracy of the analysis, they carried out experimental tests on two types of panels with polymer and metal foam cores and aluminum facesheets, revealing that the analytical method provided acceptable accuracy. Hou et al. (2010) studied the penetration at quasi-static loading and ballistic impact of metal sandwich structures with aluminum foam core. They analyzed the effects of initial velocity, projectile geometry, thickness and density of the foam core on ballistic limit velocity and energy absorption. The results showed that energy absorption and ballistic limit velocity were enhanced by increasing the initial velocity of the projectile, thickness of the sandwich structure and density of the foam. Dean et al. (2011) studied numerically and experimentally the energy absorption during penetration of the projectile into a sandwich structure with a metal fiber core. The experimental results showed that the rate of energy absorption was máximum at velocities close to the ballistic limit velocity. Furthermore, the numerical analysis showed that such increase originated from the kinetic energy of separated particles and somewhat related to the strain rate effect.

Cao et al. (2015) evaluated the performance of shock energy absorption in sandwich structures with combined aluminum honeycomb core under impact loads. They suggested that combined honeycomb structure has more energy absorption capacity than a single honeycomb.

Nasirzadeh and Sabet (2014) examined the ballistic limit and energy absorption of sandwich structures with polyurethane foam core and investigated the effect of nanoclay of the polyurethane foam core on impact properties of sandwich structures. Ghalami-Choobar and Sadighi (2014) studied numerically and experimentally the effects of many parameters including projectile velocity, core density, core thickness, facesheet thickness and orientation of fibers on the ballistic behavior and

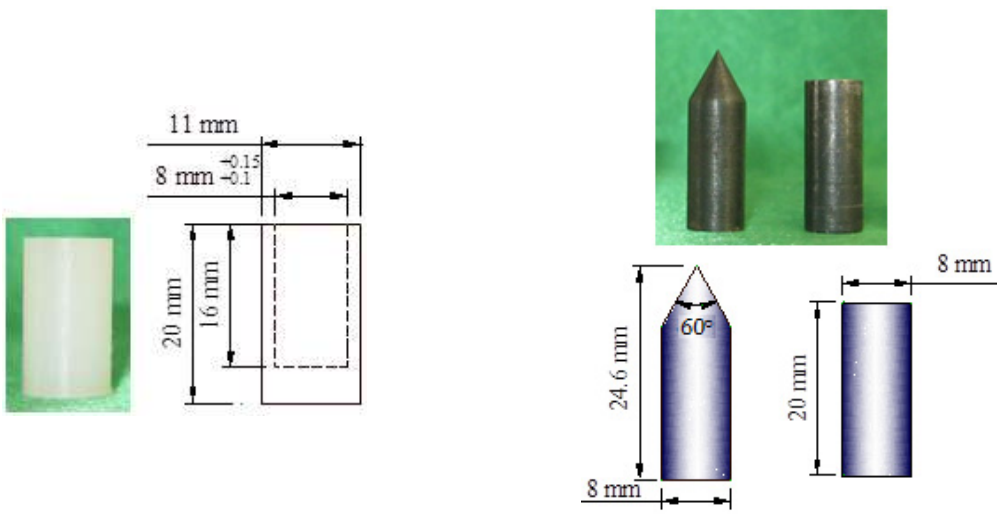
energy absorption of sandwich structures with polyurethane foam core, aluminum and composite facesheets.

The current study intended to conduct ballistic tests on sandwich structures with aluminum facesheet and polymer foam core, so as to examine the effect of several parameters such as impact velocity, density variations of the core, projectile nose shape and reinforcement of foam core through aluminum pins on ballistic limit and energy absorption.

2 EXPERIMENTAL TESTS

2.1 Material Properties

Projectile: The projectiles used for experimental tests had a length of 20 mm, diameter of 8 mm, and mass of 7.92 g made of steel (VCN) hardened to 52 Rockwell (Figure 1 and Table 1). The projectile nose shapes was flat and conical so as to examine its effect on the ballistic limit and energy absorption.



a) Sabot b) Projectiles

Figure 1: Geometry of sabot and projectiles.

Mechanical properties	Data
ρ (kg/m^3)	7860
E (GPa)	210
ν	0.3

Table 1: Material properties of the projectiles.

Facesheets: The 5005-H16 aluminum facesheets were selected for sandwich specimens. Tensile tests were conducted to specify the stress-strain curve (Figure 2) on three specimens according to ASTM-E8 with Instorn-5500r apparatus. The mechanical properties of aluminum facesheets are listed in Table 2.

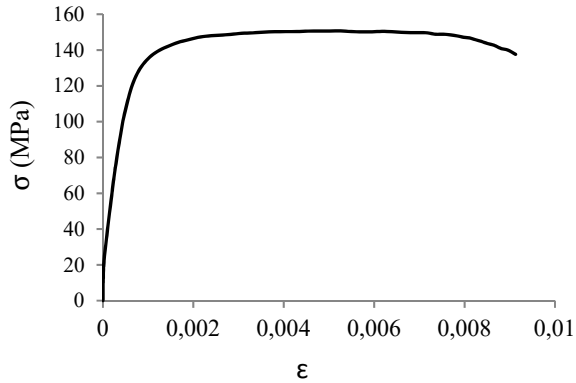


Figure 2: The tensile stress-strain curve for aluminum sheets Al-5005H16.

Material	Thickness, h_f (mm)	Density, ρ (kg/m^3)	Young's modulus, E (GPa)	Poisson's ratio, ν	Tensile strength, σ_y (MPa)	Fracture strain, ε_f
Al-5005H16	1.5	2700	70.04	0.3	145.5	0.009

Table 2: Material properties of the facesheets.

Aluminum pins: Aluminum pins used in the core of sandwich structures were made of pure aluminum (99%) with a diameter of 2 mm and length of 30 mm. The pins are distributed whitin the polyurethane foam core based on an irregular arrangement.

Polyurethane foam: The core of sandwich structures were made of polyurethane foam with closed cells at densities of 248, 359 and 600 kg/m^3. The mechanical behavior of foam was identified through standard ASTM D1621-00 (Chen, Lu et al. 2002). The results of tests for axial compression of foams and their mechanical properties have been displayed in Figure 3 and Table 3, respectively.

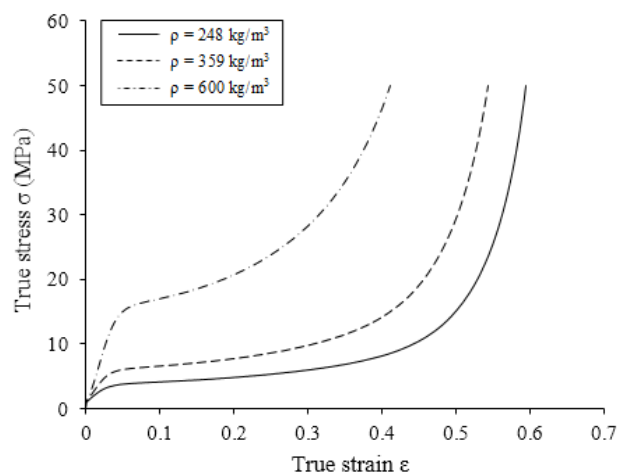


Figure 3: Compressive curve for polyurethane foams based on standard ASTM D1621-00.

Density, ρ (kg/m^3)	Young's modulus, E(MPa)	Poisson's ratio, ν	Plateau stress, σ_{pl} (MPa)	Densification strain, ε_D
248	102	0.33	5.75	0.57
359	154.2	0.33	7.96	0.53
600	370.6	0.33	17.72	0.36

Table 3: Material properties of the foams.

2.2 Fabrication of Specimens

The tested sandwich structures consisted of two aluminum facesheets with polyurethane foam core or composite core (polyurethane foam reinforced with aluminum pins). The facesheets were 1.5 mm thick, while the specimens with foam core were prepared at densities of 248, 359 and 600 kg/m^3 and thicknesses of 22, 35 and 50 mm, respectively. Moreover, the composite core specimens were constructed at pin-foam weight ratios of 37% and 63%. The specimens were prepared at dimensions of 100×100 mm squares as many as 14 samples for each case. The facesheets were glued to the core through Epoxy adhesive. Therefore, five different types of specimens were tested: three types with polyurethane foam cores having 248, 359 and 600 kg/m^3 densities, respectivly; and two types with pin reiforced polyurethane cores with pin-foam weight ratios of 37% and 63%. For each type 14 specimens were made (a total of 70 specimens) which 1/2 of them were subjected to impact of blunt nose projectiles, whereas the reminder tested by conical nose projectiles. Figure 4 illustrates two of the specimens, and Tables (4 and 5) display the physical properties of the samples.



A) Sandwich specimen with polyurethane foam core **B)** Sandwich specimen with composite core

Figure 4: Isometric view of sandwich specimens with aluminum facesheets.

Coding of specimens: Codes P248, P359 and P600 are used for polyurethane foam core specimens and the three-digit number represents the density of foam, while AP37 and AP63 denoted to composite core specimens and the two-digit number represents the weight percentage of aluminum pin in the foam core. The right-hand side letter represents the shape of projectile nose used in impact tests (C for conical nose and B for blunt-head). These codes are presented in Tables 4 and 5, respectively.

Specimen name	Core density (kg/m^3)	Core thickness (mm)	Facesheet thickness (mm)
P248B, P248C	248	50	1.5
P359B, P359C	359	35	1.5
P600B, P600C	600	22	1.5

Table 4: The codes assigned to each specimen with polyurethane core.

Specimen name	Core density (kg/m^3)	Mass of foam in core (gr)	Mass of aluminum pin in core (gr)
AP37B, AP37C	460	79	46
AP63B, AP63C	457	46	79

Table 5: The codes assigned to each specimen with composite core.

2.3 Ballistic Tests

This section discusses the penetration experiments on rigid conical nose and blunt-head projectiles in sandwich structures, so as to evaluate the effect of projectile velocity, core density and pin aluminum wt% in polyurethane foam core on ballistic resistance of the targets. The ballistic tests were conducted through single-stage gas gun (Figure 5). In order to measure the velocity of the projectile before hitting the target, a stopwatch equipped with optical and digital counter was employed. In order to measure residual velocity, the velocity of the projectile after impact, two parallel two-dimensional screens from a laser light source and photodiode were employed each containing 80 laser light source in both horizontal and vertical directions. Figure (6) illustrates the measurement system used in the impact tests.

The specimens were kept tight through screws in the chamber of the gas gun, so that completely clamped boundary conditions were met at the edges of the sandwich structure. The effective surface of sandwich structure against projectile in the chamber was a square with a side of 80 mm.

After placing the specimen in a special fixture and setting the pressure of the tank, the projectile was fired toward the target. The velocities before and after impact to the target were measured and recorded. For each specific system of projectile and target, there were 7 tests. For 10 projectile-target systems, there were a total of 70 experiments, the data of which were adopted to draw the residual velocity versus impact velocity curves.

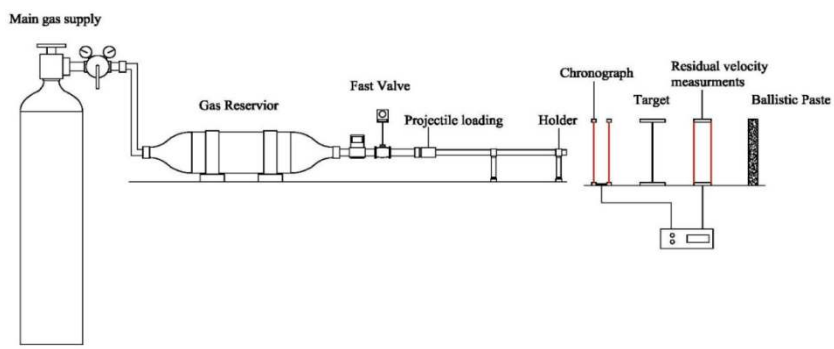


Figure 5: Schema of gas gun.

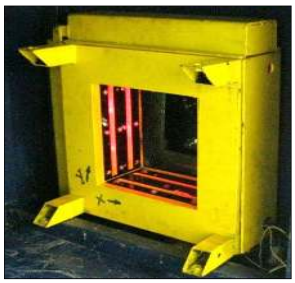


Figure 6: The measurement system for residual velocity.

3 RESULTS AND DISCUSSION

This section represents the results of ballistic tests and the effect of several parameters such as impact velocity, variation of thickness and density of the core, reinforcement of foam core through aluminum pins at different weight percentages by as well as the shape of projectile nose on the ballistic limit and energy absorption. Moreover, comparison was made between the energy absorption and ballistic limit of different types of targets.

3.1 Effect of Impact Velocity

Figure (7) illustrates the changes in residual velocity of the projectile at different initial velocities for the foam core with density of 248 kg/m^3 (P248B and P248C types). According to the ballistic limit curves, as initial velocity increases, the residual velocity increases too; this curve is non-linear within the area close to the ballistic limit velocity V_b, whereas it tends to be almost linear in the last part. This trend is similar to the ballistic limit curves for composite sheets (Nasirzadeh and Sabet 2014).

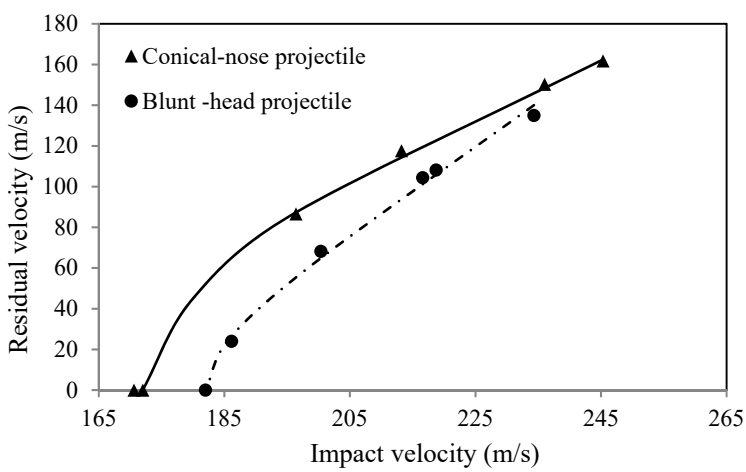
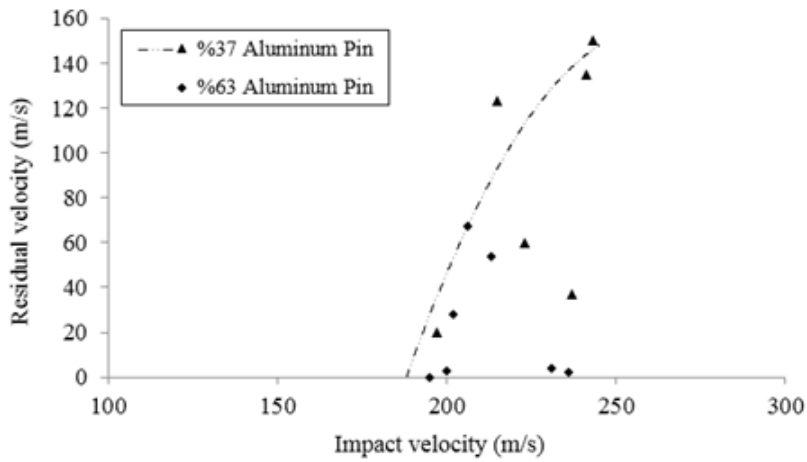
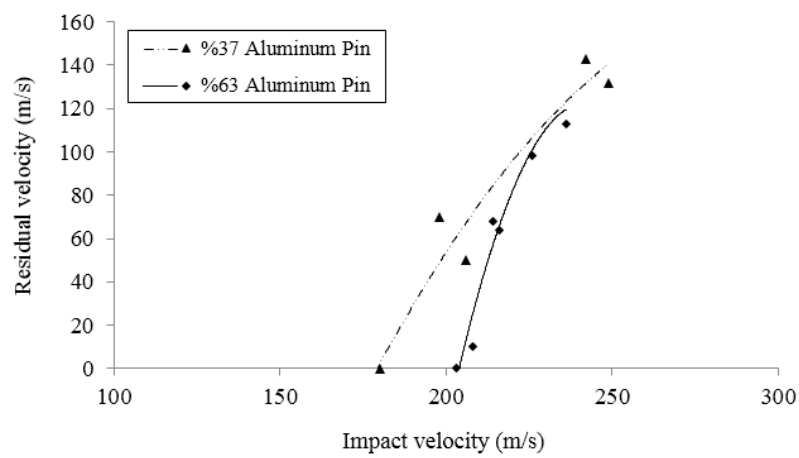


Figure 7: The curve for variations of residual velocity versus the initial velocity for sandwich structures with foam core density of 248 kg/m^3 (blunt-head projectile and conical-nose projectile).

Figure (8) illustrates the changes in residual velocity of the projectile at different initial velocities for the composite core specimens with different weight percentages of the aluminum pins. At identical initial velocities, as the percentage of aluminum pins increases, there will be lower residual velocity in the specimens. It can therefore be stated that increase in the percentage of pins can decrease the residual velocity, thus improves the ballistic resistance of the structure. As seen in the figures, the ballistic limit velocity was similarly influenced by the percentage of pins used in the composite core structures. The sandwich specimen with 63 wt% of aluminum pins had the highest ballistic limit compared with other composites. As can be seen in the experimental results of blunt-head projectile impact, there are discrepancies at both composite specimens, which is attributed to the distribution of pins in the core and the effect of projectile nose shape. However, there is no such trend found in the results of conical nose projectile impact. This is because of pins dispersed by conical nose projectile during penetration as well as the deformation of pins against the conical nose projectile.



A) blunt-head projectile



B) conical-nose projectile

Figure 8: Variations of residual velocity versus the initial velocity for AP63 and AP37 sandwich structures.

According to the Figures 7 and 8, it is clear that the ballistic limit of specimens impacted by blunt-nose projectile had a random mode, so that the ballistic limit at minimum was obtained for sandwich specimen with polyurethane foam core (200 m/s) and at minimum for sandwich specimens with 63 percent pins at 236 m/s for blunt-nose projectile. The figures indicate that as the weight percentage of pins increased, there was a significant growth in ballistic resistance of composite core specimens, however the amount of increase is not predictable since it depends on the percentage of pins hitted by the projectile.

Figure 9 shows that an increase at impact velocity results in increase of absorbed energy; actually, this behavior is related to the effect of loading rate or strain rate. The numerical examinations by Dean et al. (2011), Ghalami-Choobar and Sadighi (2014) on sandwich structures with metal facesheets similarly indicated such a behavior; they have stated that the curve has a relative extremum for energy absorption close to the ballistic limit velocity.

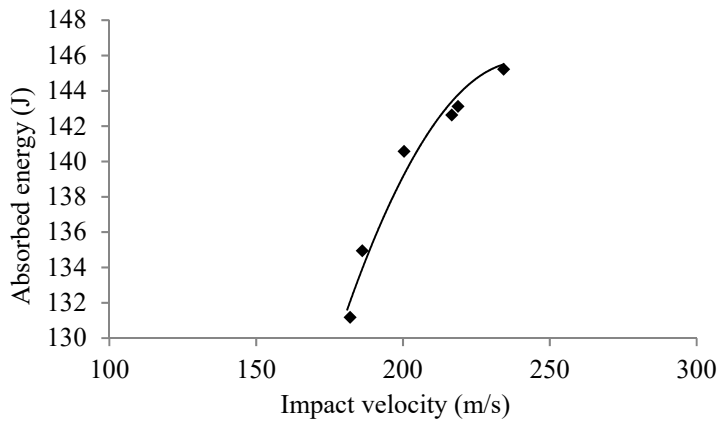


Figure 9: Variation of absorbed energy versus initial velocity of the projectile for sandwich specimen P248B.

According to Figure (10), as the initial velocity of the projectile increases from 216.6 to 234.3 m/s, there will be increase in the energy absorption of tested sandwich structures with blunt-head projectile by 1.82%, 2.53% and 3.33%, respectively, for densities of 248, 359 and 600 kg/m3. Besides, this figure shows that the energy absorption of sandwich structures increases with increased density of the foam. With 142 percent increase in density of polyurethane foam core, energy absorption of sandwich structure increases by 62% for the blunt projectile and 48% for conical nose projectile. Thus, the density increase with decreasing thickness of the foam, is the perfect option to increase the energy absorption of sandwich structures with aluminum surfaces.

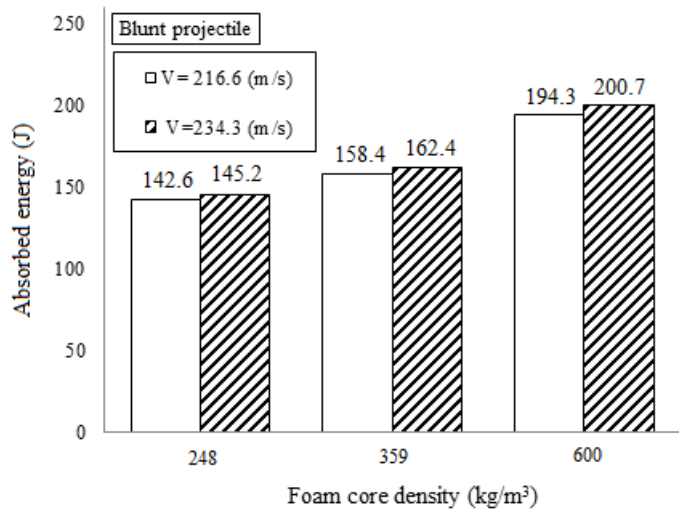


Figure 10: Comparison of absorbed energy by sandwich structures with different core densities impacted by blunt-head projectile.

3.2 Effect of Core Density

Figure (11) shows the variations of ballistic limit velocity with foam density of sandwich specimens. According to this figure, there is a nearly linear relationship between the ballistic limit velocity and core density. This relationship was consistent with the results of Hou et al. (2010), Ghalami-Choobar and Sadighi (2014). Table (6) compares linear and exponential equations fitted to the results of the present study with those of references Hou et al. (2010) and Cao et al. (2015) for predicting the behavior of sandwich structures versus density. This table shows that the exponential relationship obtained through Excel calculations was y=54.78x^0.217, represents a better prediction for the behavior of sandwich structures.

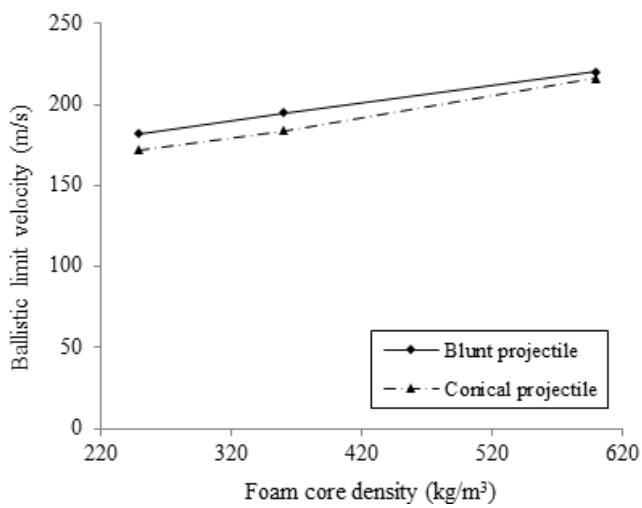


Figure 11: variation of ballistic limit velocity versus foam density in sandwich specimens.

Data used	R-square			RSME		
	Present	Hou et al. [2010]	Ghalami & Sadighi [2014]	Present	Hou et al. [2010]	Ghalami & Sadighi [2014]
Linear law (ax+b)	0.9894	0.9436	0.9866	10.30	10.93	9.074
Power low (ax^b+c)	0.9954	0.9805	1.0000	0.108	0.3426	0.0013

Table 6: Comparison of predictive relationship for behavior of sandwich structures versus the density of core foam.

Figure (12) indicates the absorbed energy versus density at impact velocity of 236 m/s. It also shows that energy absorption varies at different densities, where specimen P600B exhibited maximum energy absorption. According to Figure (13), the energy absorption of sandwich structures is enhanced at higher foam densities. As the density of polyurethane foam core increases by 141.93%, the energy absorption of sandwich structures varied for blunt-head projectile by 38.62% and for conical nose projectile by 48.5%. Hence, increased density together with decreased thickness of the polyurethane foam can be ideal for enhancing the energy absorption of sandwich structures with aluminum facesheets.

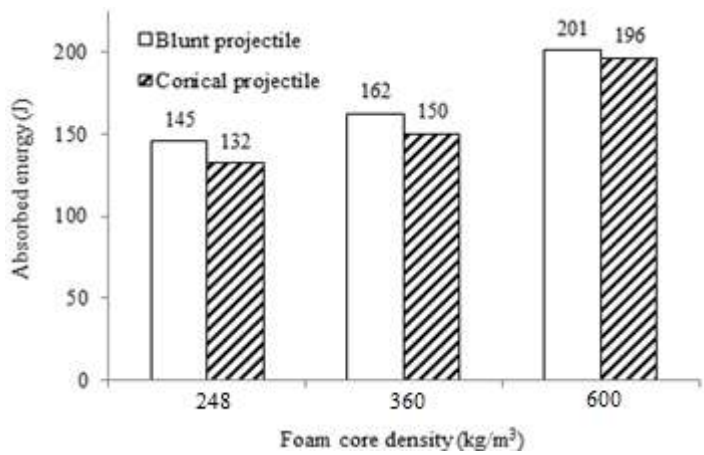


Figure 12: Comparison of energy dissipation versus core density of sandwich structures at impact velocity of 234.3 m/s.

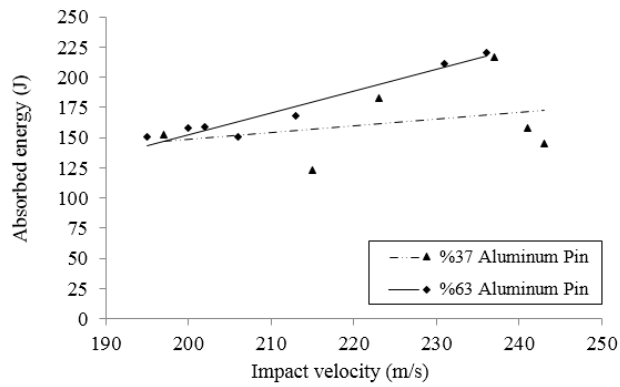
3.3 Effect of wt% of Pins

The absorbed energy during full penetration of the projectile was calculated through the data concerning the initial and residual velocities. Figure (13) illustrates the changes of energy absorption with the weight percentage of the pins inside the core. The energy absorbed by sandwich structures was calculated based on the principle of conservation of energy.

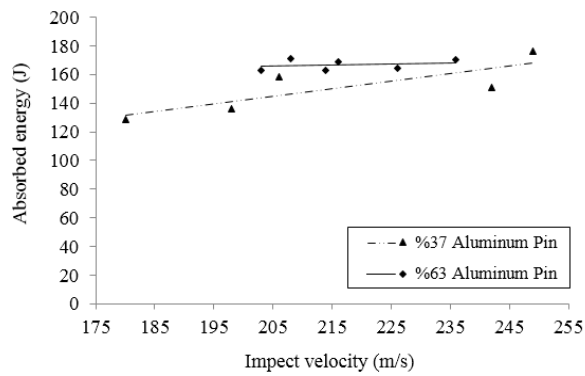
According to these figures, there is an obvious effect of increases pins on the energy absorption of specimens with composite core. Moreover, there is an obvious upward trend in energy absorption by up to 63% of pin weight. In fact, the best ballistic properties at 63% weight of pin occurred against specimens with 37 wt% pins. This behavior can be explained primarily by the addition of aluminum

pins to the foam, raising the modulus of specimens, thus delaying the initial stage of foam failure. Secondly, it can be argued that the involvement of pins inside the specimens altered the failure path, thus delaying the growth stage of the crack, which ultimately improved the impact properties of specimens. Examination on the core of sandwich structures in different weight percentages of pins indicated that brittleness of foam is curtailed at higher percentage of pins in the foam. In addition, the evaluation of the specimens after high-velocity impact test showed that a certain portion of the foam was cutoutted and exits with the projectile from the specimen, leading to rupture and widening of the petal surface. Subsequently, there was a hole within the foam of sandwich structures.

According to Figure (14) as the initial velocity of the projectile increases, there was a relative increase in the energy absorption of specimens at different pin percentages. This behavior can be associated with higher strain rate as initial velocity of projectile increased. Previous research in this regard indicated that capability of energy absorption in sandwich structures was enhanced when impact velocity was increased (Mines, Worrall et al. 1998, Buitrago, Santiuste et al. 2010, Nasirzadeh and Sabet 2014).



A) blunt-head projectile

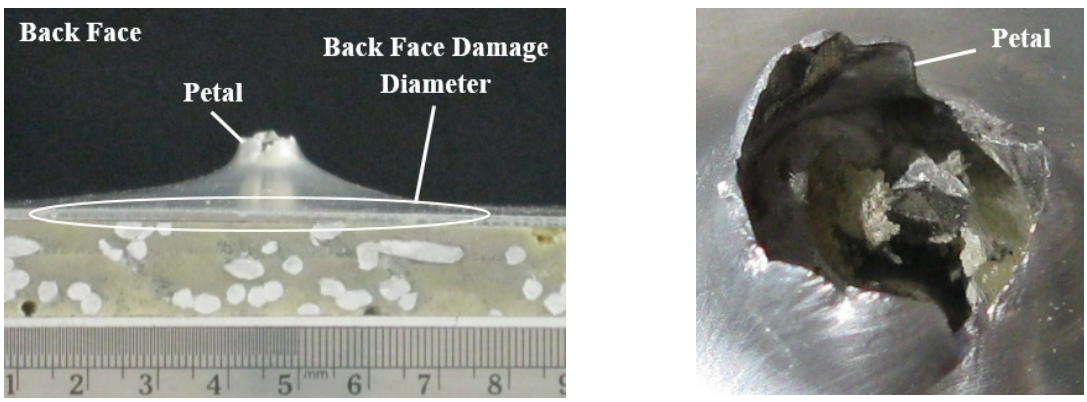


B) conical-nose projectile

Figure 13: The energy absorption versus the initial velocity for specimens with different percentages of aluminum pins

3.4 Evaluation of Structural Damage

The failure mechanism for all of the specimens involved shear plug on the impact side facesheet, petalling and dishing on the opposite side, which somehow confirmed the type of damage to the sandwich panels with aluminum facesheets. This was previously reported by other researchers (Hoo Fatt and Park (2001), García-Castillo, Buitrago et al. (2011)). Figure 14 displays a side view of the sandwich panels with composite core and a more accurate picture of the region of the projectile exit. In this figure, the extent of damage zone has been specified on the surface of the rear facesheet.



A) Side view of the tested specimen

B) Projectile exit zone

Figure 14: The rear facesheets damage in specimen AP63C1 tested at initial velocity of 243 m/s.

3.4.1 Evaluation of the Damage at Specimens with Foam Core

Figure (15) indicates the diameter of the rear facesheet damage in P248 impacted with blunt-head and conical nose projectiles versus initial velocity. This figure shows that as the initial velocity increases, the diameter of the damaged área decreases. At higher velocities and adequately higher than the ballistic limit, the diameter follows a steady linear trend, which is an expected behavior. With increasing velocity and consequently increasing kinetic energy, the penetration of the projectile in the sandwich structure becomes more local. In such circumstances, there is little opportunity for deformation and widening of the holes. The important point in this graph is the difference between the damage area caused by blunt-head and conical nose projectiles, proving the effect of the geometry of projectile on the damage of rear facesheet. It should be noted, however, the deflection and rotation of the projectile in this specimen were low. Obviously, if the projectile entails dome deflection and rotation, then there will be greater diameter of the damaged area. In fact, it can be stated that there is a direct relationship between the diameter of the damaged zone and the absorbed energy. The wider the range of damage, the greater the amount of energy absorption.

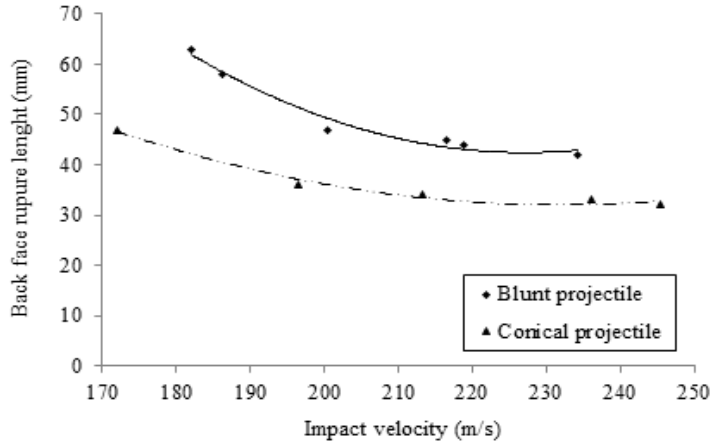
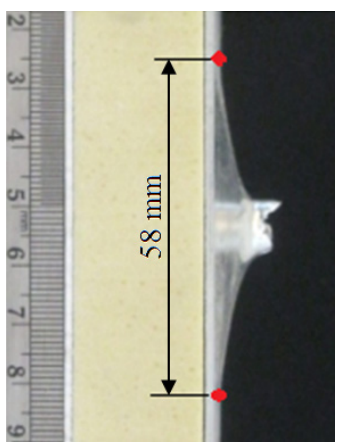
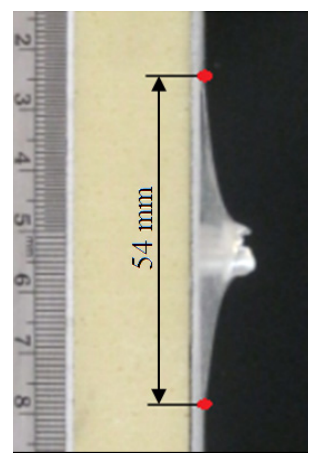


Figure 15: Damage at the rear facesheet for specimen with density of 248kg/m3 at different velocities.

Pictures of the damage and dishing of the rear surface of sandwich samples with the same core density of 600 kg/m3 at two different residual velocities are shown in Figure 16. Damages show that at higher residual speeds, dishing zone is smaller and created petals are regular with small dimensions, this behavior proves local penetration at high velocities. Also according to Figure 17 that shows two similar sandwich panel impacted at speeds of 200 and 235 m/s the effect of velocity on the dorsal surface damage can be investigated. The figure declares that with greater initial velocity the number of petals increases but their dimensions is decreased.

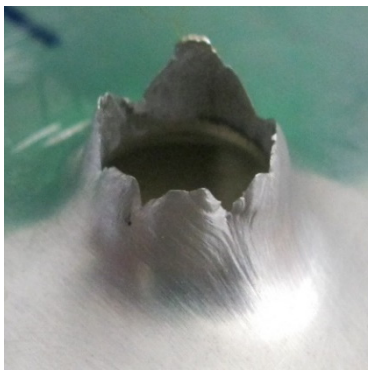


A) The area of rear facesheet damage for specimen P600B2 at residual velocity of 70.2 m/s

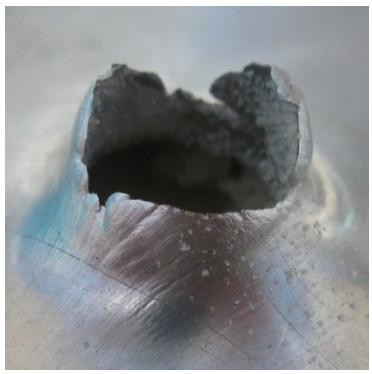


B) The area of rear facesheet damage for specimen P600B6 at residual velocity of 103 m/s

Figure 16: Images of damage to rear facesheet of sandwich specimens with foam core.



A) Impact velocity 235 m/s



B) Impact velocity 200 m/s

Figure 17: Effect of initial velocity on the rear face-sheet damage at P248B7 sample.

3.4.2 Damage in Specimens with Composite Core

The measuring of holes created in the specimens with composite core showed that the diameters of front and rear areas in specimens with 37 and 63 weight percentages of pins were equal in most cases and nearly equal to the diameter of the projectile; in cases where pins at the site of projectile penetration led to deflection and rotation of the projectile during penetration, slightly widening the diameter of the hole is seen. In the cases which the back hole is slightly greater, this difference increases as the pin percentage increases. In the case of the composite core specimens, there were a little rotation and deflection of the projectile, which can be explained by the smaller thickness of the specimens. By investigating the damaged area of the specimens, it was found out that if the compaction of pins is low along with the penetration line of the projectile, penetration occurs without any deflection and rotation, given the high velocity of projectile and consequently low energy dissipation. With increasing percentage of pins along the penetration path of the projectile, the pins enhance the foam resistance, thus altering the course of projectile motion detected in several specimens. In general, the damage at the front facesheet in specimens with composite core was similar to that of sandwich specimens with foam core.

There was a different trend concerning damage to the rear facesheet. For specimens with 37 wt% of aluminum pins in collision with conical nose projectile, the dishing and petals were similar to those obtained for cores without pins. It seems that due to low percentage of pins, the structure failed to resist against conical nose projectiles and the pins across the penetration path were shoved aside by the projectile. Nevertheless, the energy absorption in these specimens was higher than that in pin-free specimens because of the projectile energy spent partially to shove aside the pins involving a compressive force on the foam and crushing the aluminum pins. In these specimens, the damaged area shrinks with increasing velocity, indicating that the damaged area becomes local at higher velocities.

In specimens with 37 wt% of aluminum pins in collision with blunt-head projectile and specimens were with 63 wt% of aluminum pins with blunt-head and conical nose projectiles, there were rupture in the rear facesheet as well as the projectile discharge zone, isolation of pin and foam and inadequate cohesion between the two and also a little tenderness and crushed foam. The involvement of pins in

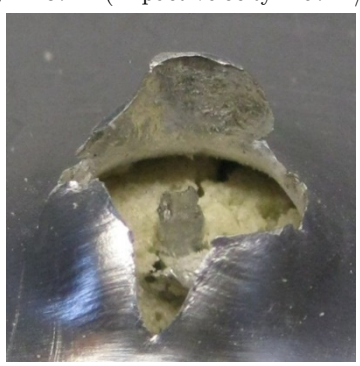
the core of sandwich structures reflected different deformations in the rear facesheet. In certain cases, the pins bent away and deflected from the motion path. In other cases, there were crushing and rupture. As stated earlier, the projectile exit from the rear facesheet created petal and dishing. In specimens with composite core, if the pins are arranged in front of the projectile, then there will be rupture on the rear facesheet of the petal zone. In specimens with this type of shear damage, the energy absorption tends to increase more intensely, indicating it has been spent partially on creating a rupture on the aluminum facesheet. The damage to the rear facesheet and exit zone of the projectile for sandwich specimens with composite core is shown in Figures (18-19).



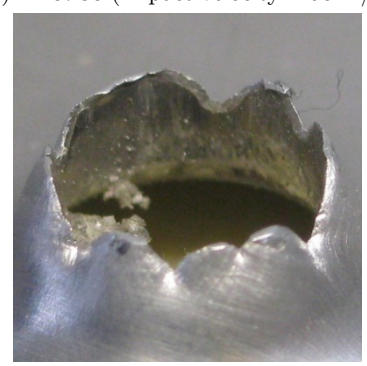
A) AP37B2 (Impact velocity=197 m/s)



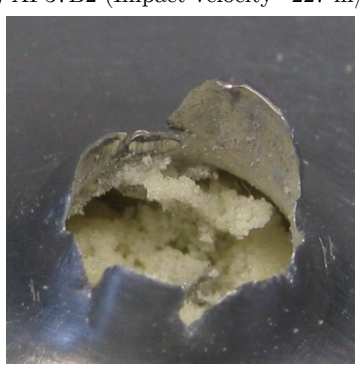
B) AP37C3 (Impact velocity=198 m/s)



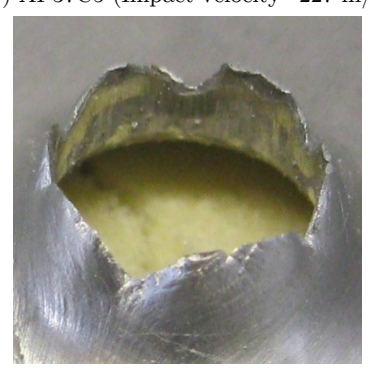
C) AP37B2 (Impact velocity=227 m/s)



D) AP37C5 (Impact velocity=227 m/s)

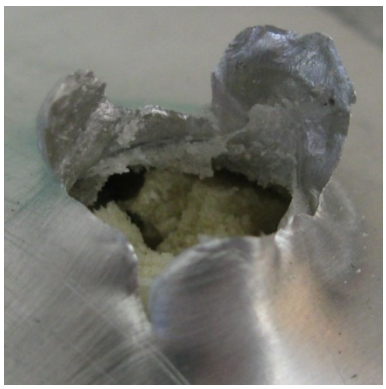


E) AP37B6 (Impact velocity=243 m/s)



F) AP37C6 (Impact velocity=242 m/s)

Figure 18: Compare damage and petals shape of the rear face-sheet of sandwich panels with 37% pin tested with blunt and conical nose projectiles at the same initial velocities



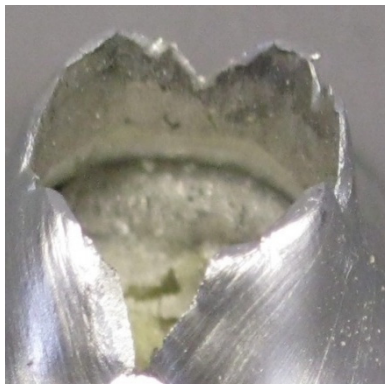
A) AP63B1 (Impact velocity=236 m/s)



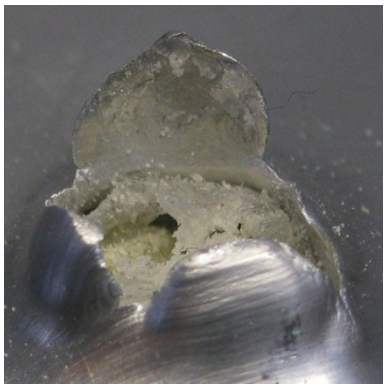
B) AP63C6 (Impact velocity=236 m/s)



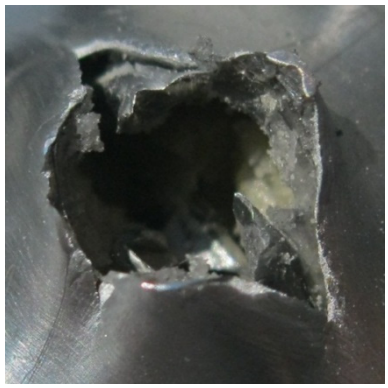
C) AP63B2 (Impact velocity=213 m/s)



D) AP63C7 (Impact velocity=214 m/s)



E) AP63B6 (Impact velocity=206 m/s)



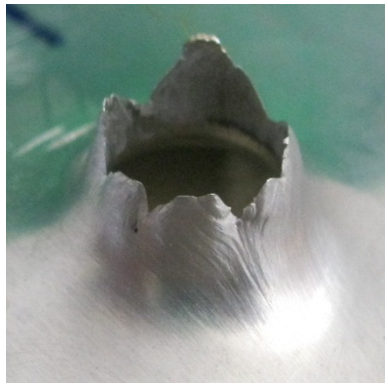
F) AP63C5 (Impact velocity=208 m/s)

Figure 19: Compare damage and petals shape of the rear face-sheet of sandwich panels with 63% pin tested with blunt and conical nose projectiles at the same initial velocities.

3.5 Effect of the Projectile Nose Shape

The rear surface damage of sandwich samples can be evaluated through study of created petals and dishing zone dimension. Picture of sandwich samples with different core densities, is shown in Figure 20. The images show that the rear surface damage depends on the type and velocity of projectile.

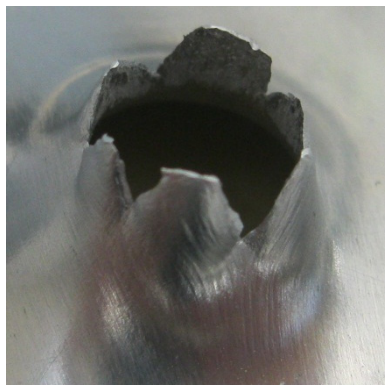
Blunt projectile leads to fewer and larger number of petals, whereas conical nose projectile resulted in a more number and smaller dimension petals.



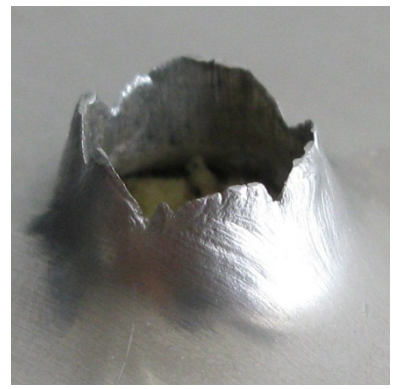
A) P248B1 (Impact velocity=236 m/s)



B) P248C2 (Impact velocity=236 m/s)



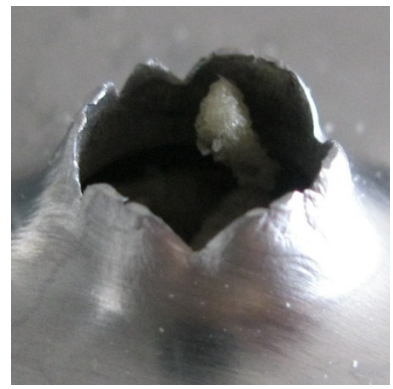
C) P359B4 (Impact velocity=233 m/s)



D) P359C3 (Impact velocity=233 m/s)



E) P600B2 (Impact velocity=236 m/s)



F) P600C6 (Impact velocity=236 m/s)

Figure 20: The damage zone and petals in different density foam core sandwich specimens impacted by blunt and conical nose projectiles.

Ballistic limit velocities of sandwich panels with different core densities, impacted with projectiles are compared in Table 7. As is clear the ballistic limit of these panels is greater in dealing with blunt projectile compared with conical nose projectile, and this is due to increased energy absorption of sandwich panels in a collision with a blunt projectile.

Core density	Ballistic limit		Differencec(%)
	Conicalc-nose projectile	Blunt-head projectile	
248	172	182	5.4 %
360	184	195	5.6 %
600	216	220.2	1.9 %

Table 7: Effect of projectile nose shape on the ballistic limit velocity.

Ballistic limit velocity and energy absorption: Based on the results of high-velocity impact tests, the ballistic limit velocity and energy absorption during penetration into sandwich structures were calculated and then presented below.

A) In specimen with core density of 248 kg/m^3: The blunt-head projectile led to 11.96% higher energy dissipation and 5.4 % increase in ballistic limit velocity compared to the conical nose projectile.
B) In specimen with core density of 359 kg/m^3: The blunt -head projectile led to 12.31% higher energy dissipation and 5.6 % increase in ballistic limit velocity compared to the conical nose projectile.
C) In specimen with core density of 600 kg/m^3: The blunt -head projectile led to 3.96% higher energy dissipation and 1.9 % increase in ballistic limit velocity compared to the conical nose projectile.

The test data showed that blunt -head projectile resulted in higher ballistic limit velocity and energy dissipation compared to conical nose projectile.

4 CONCLUSIONS

This study intended to empirically investigate the ballistic resistance and energy absorption of sandwich structures made of Al-5005H16 facesheets, polyurethane foam core and polyurethane foam core reinforced with aluminum pins (which is studied for the first time). There were three foam core specimens constructed at three densities of 248, 359 and 600 kg/m^3. The specimens with composite core were manually developed two weight ratios of 37 and 63 percentages of aluminum pins within foam core. For each of 5 types of specimens, 14 samples were fabricated; 7 tested with blunt nose and 7 with conical nose projectiles. The gas gun with air propellant was used at velocity range of 170- 260 m/s. According to the results, the ballistic behavior and energy absorption of sandwich structures were affected by several parameters such as foam core density, weight percentage of pins used in the core, geometry of the nose and the projectile velocity. The following explores the key results:

- In sandwich structures with foam core, increasing the core density resulted in increase at the ballistic limit velocity and energy absorption.
- Assuming a constant weight of foam core, there was an increase in density of core and decrease in the thickness in terms of ballistic limit velocity and energy absorption.

- The failure mechanism for all specimens involved shear plug on the front facesheet, petaling and dishing on the rear facesheet.
- At equal initial velocities for all specimens, the area of damage on the front aluminum facesheet was approximately equal to the diameter of the projectile, whereas the extent of damage on the rear facesheet varied at different densities, and sandwich structures with higher foam density tended to have the maximum diameter of the damaged area.
- Owing to good mechanical resistance at high foam densities, the projectile tends to deflect from its original direction and rather rotate. As a result, it hits the rear aluminum facesheet with its lateral side. Since the cross-section of the impact is large, thus energy absorption is increased.
- It was revealed that as initial velocity of the projectile increased, there was lower diameter of the damaged area (dishing) and higher energy absorption.
- The blunt-head projectile led to wider diameter of damaged area and an increased level of ballistic limit velocity and energy dissipation.
- The application of aluminum pins in the polyurethane foam core of sandwich structures brought about a considerable increase in ballistic resistance and energy absorption.
- As for sandwich structures with composite core, changes in the type of damage to the rear facesheet and rupture at the petal zone were found to be due to aluminum pins in the core.

Reference

Alavi Nia, A. and M. Kazemi (2015). "Analytical study of high velocity impact on sandwich panels with foam core and aluminum face-sheets." Journal of Modares Mechanical Engineering 15(6): 231-239.

Belingardi, G., M. P. Cavatorta and R. Duella (2003). "Material characterization of a composite–foam sandwich for the front structure of a high speed train." Composite Structures 61(1–2): 13-25.

Buitrago, B. L., C. Santiuste, S. Sánchez-Sáez, E. Barbero and C. Navarro (2010). "Modelling of composite sandwich structures with honeycomb core subjected to high-velocity impact." Composite Structures 92(9): 2090-2096.

Cao, L., Y. Lin, F. Lu, R. Chen, Z. Zhang and Y. Li (2015). "Experimental Study on the Shock Absorption Performance of Combined Aluminium Honeycombs under Impact Loading." Shock and Vibration 2015: 8.

Chen, W., F. Lu and N. Winfree (2002). "High-strain-rate compressive behavior of a rigid polyurethane foam with various densities." Experimental Mechanics 42(1): 65-73.

García-Castillo, S. K., B. L. Buitrago and E. Barbero (2011). "Behavior of sandwich structures and spaced plates subjected to high-velocity impacts." Polymer Composites 32(2): 290-296.

Ghalami-Choobar, M. and M. Sadighi (2014). "Investigation of high velocity impact of cylindrical projectile on sandwich panels with fiber–metal laminates skins and polyurethane core." Aerospace Science and Technology 32(1): 142-152.

Goldsmith, W. and J. L. Sackman (1992). "An experimental study of energy absorption in impact on sandwich plates." International Journal of Impact Engineering 12(2): 241-262.

Goldsmith, W., C. K. H. Dharan and H. Chang (1995). "Quasi-static and ballistic perforation of carbon fiber laminates." International Journal of Solids and Structures 32(1): 89-103.

Guoqi, Z., W. Goldsmith and C. K. H. Dharan (1992). "Penetration of laminated Kevlar by projectiles—I. Experimental investigation." International Journal of Solids and Structures 29(4): 399-420.

Hoo Fatt, M. S. and K. S. Park (2001). "Dynamic models for low-velocity impact damage of composite sandwich panels – Part A: Deformation." Composite Structures 52(3–4): 335-351.

Hou, W., F. Zhu, G. Lu and D.-N. Fang (2010). "Ballistic impact experiments of metallic sandwich panels with aluminium foam core." International journal of impact engineering 37(10): 1045-1055.

J. Dean, A. S-Fallah, P. M. Brown, L. A. Louca and T. W. Clyne (2011). "Energy absorption during projectile perforation of lightweight sandwich panels with metallic fibre cores." Composite Structures 93(3): 1089-1095.

Kepler, J. (2004). "Impact Penetration of Sandwich Panels at Different Velocities - An Experimental Parameter Study: Part I - Parameters and Results." Journal of Sandwich Structures and Materials 6(4): 357-374.

Kepler, J. (2004). "Impact Penetration of Sandwich Panels at Different Velocities – An Experimental Parameter Study: Part II – Interpretation of Results and Modeling." Journal of Sandwich Structures and Materials 6(5): 379-397.

Mines, R. A. W., C. M. Worrall and A. G. Gibson (1998). "Low velocity perforation behaviour of polymer composite sandwich panels." International Journal of Impact Engineering 21(10): 855-879.

Mitrevski, T., I. H. Marshall, R. Thomson, R. Jones and B. Whittingham (2005). "The effect of impactor shape on the impact response of composite laminates." Composite Structures 67(2): 139-148.

Nasirzadeh, R. and A. R. Sabet (2014). "Study of foam density variations in composite sandwich panels under high velocity impact loading." International Journal of Impact Engineering 63: 129-139.

Reddy, T. Y., H. M. Wen, S. R. Reid and P. D. Soden (1998). "Penetration and Perforation of Composite Sandwich Panels by Hemispherical and Conical Projectiles." Journal of Pressure Vessel Technology 120(2): 186-194.

Reyes, A., O. S. Hopperstad, T. Berstad, A. G. Hanssen and M. Langseth (2003). "Constitutive modeling of aluminum foam including fracture and statistical variation of density." European Journal of Mechanics - A/Solids 22(6): 815-835.

Roach, A. M., K. E. Evans and N. Jones (1998). "The penetration energy of sandwich panel elements under static and dynamic loading. Part I." Composite Structures 42(2): 119-134.

Roach, A. M., N. Jones and K. E. Evans (1998). "The penetration energy of sandwich panel elements under static and dynamic loading. Part II." Composite Structures 42(2): 135-152.

Tan, V. B. C. and K. J. L. Khoo (2005). "Perforation of flexible laminates by projectiles of different geometry." International Journal of Impact Engineering 31(7): 793-810.